Controller and Estimator Design for Regulation of Film Thickness, Surface Roughness, and Porosity in a Multiscale Thin Film Growth Process

Xinyu Zhang,[†] Gangshi Hu,[†] Gerassimos Orkoulas,[†] and Panagiotis D. Christofides*[,†,‡]

Department of Chemical and Biomolecular Engineering, University of California, Los Angeles, California 90095, and Department of Electrical Engineering, University of California, Los Angeles, California 90095

This work focuses on simultaneous regulation of film thickness, surface roughness, and porosity in a multiscale model of a thin film growth process using the inlet precursor concentration as the manipulated input. Specifically, under the assumption of continuum, a partial differential equation model is first derived to describe the dynamics of the precursor concentration in the gas phase. The thin film growth process is modeled via a microscopic kinetic Monte Carlo simulation model on a triangular lattice with vacancies and overhangs allowed to develop inside the film. Closed-form dynamic models of the thin film surface profile and porosity are developed and used as the basis for the design of model predictive control algorithms to simultaneously regulate film thickness, surface roughness, and porosity. Both state feedback and porosity estimation-based output feedback control algorithms are presented. Simulation results demonstrate the applicability and effectiveness of the proposed modeling and control approach by applying the proposed controllers to the multiscale model of the thin film growth process.

1. Introduction

Modeling and control of thin film microstructure in thin film deposition processes has attracted significant research attention in recent years. Specifically, kinetic Monte Carlo (kMC) models based on a square lattice and utilizing the solid-on-solid (SOS) approximation for deposition were initially employed to describe the evolution of film microstructure and design feedback control laws for thin film surface roughness.[1,2] Furthermore, a method that couples partial differential equation (PDE) models and kMC models was developed for computationally efficient multiscale optimization of thin film growth.[3] However, kMC models are not available in closed-form and this limitation restricts the use of kMC models for system-level analysis and design of model-based feedback control systems.

Stochastic differential equations (SDEs) arise naturally in the modeling of surface morphology of ultrathin films in a variety of thin film preparation processes.[4−8] Advanced control methods based on SDEs have been developed to address the need of model-based feedback control of thin film microstructure. Specifically, methods for state/output feedback control of surface roughness based on linear[9−11] and nonlinear[12,13] SDE models have been developed.

In the context of modeling of thin film porosity, kMC models have been widely used to model the evolution of porous thin films in many deposition processes.[14−17] Deterministic and stochastic ordinary differential equation (ODE) models of film porosity were recently developed[18] to model the evolution of film porosity and its fluctuation and design model predictive control (MPC) algorithms to control film porosity to a desired level and reduce run-to-run porosity variability. More recently, simultaneous control of film thickness, surface roughness, and porosity within a unified control framework was addressed on the basis of a kMC thin film growth model using the deposition rate as the manipulated input.[19] However, in a practical thin film growth setting, the surface deposition rate cannot be manipulated directly but indirectly through manipulation of the inlet precursor concentration.

The present work addresses this practical consideration and focuses on simultaneous regulation of film thickness, surface roughness, and porosity in a multiscale model of a thin film growth process using the inlet precursor concentration as the manipulated input. Specifically, under the hypothesis of a continuum, a partial differential equation model is used to describe the dynamics of the precursor concentration in the gas phase. The thin film growth process is modeled via a microscopic kinetic Monte Carlo simulation model on a triangular lattice with vacancies and overhangs allowed to develop inside the film. The macroscopic and microscopic models are connected through boundary conditions. Distributed parameter and lumped dynamic models are developed to describe the evolution of the film surface profile and porosity, respectively. The developed dynamic models are then used as the basis for the design of state and output feedback model predictive control algorithms to simultaneously regulate film thickness, surface roughness, and porosity. Simulation results demonstrate the applicability and effectiveness of the proposed modeling and control approach by applying the proposed controllers to the multiscale process model.

2. Preliminaries

We consider a silicon thin film growth process in a low-pressure chemical vapor deposition (LPCVD) reactor, which is shown in Figure 1. Due to the large discrepancies of the time and length scales between the gas-phase and the thin-film growth phenomena, two different models are employed to describe the evolutions of the gas phase and of the thin film. Under the hypothesis of continuum, a PDE model derived from a mass balance is used to describe the precursor concentration in the gas-phase. The thin film growth model is simulated through an on-lattice kMC model that uses a triangular lattice and allows overhangs and vacancies to

* To whom correspondence should be addressed: E-mail: pdc@seas.ucla.edu. Phone: +1(310)794-1015. Fax: +1(310)206-4107.
[†] Department of Chemical and Biomolecular Engineering.
[‡] Department of Electrical Engineering.

10.1021/ie901396g
Published on Web 11/12/2009

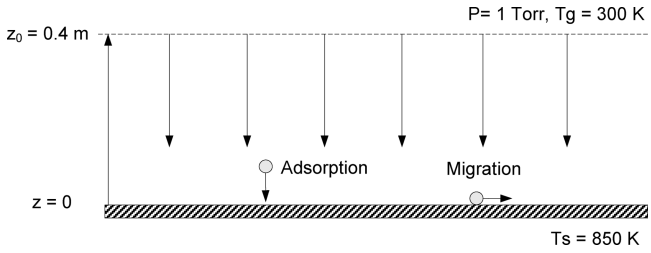

Figure 1. Schematic of thin film growth process in an LPCVD reactor.

Table 1. Gas-Phase Model Parameters

T_g	300 K	P	1 torr
T_s	850 K	z_0	0.4 m
c_0	−2.90	K	0.5
c_1	2.06×10^{-2}	K_H	0.19 $Pa^{-1/2}$
c_2	2.81×10^{-5}	K_s	0.70 Pa^{-1}

develop inside the film. The two models are connected through boundary conditions, i.e., the adsorption rate in the kMC model depends on the reactant concentration right above the surface following an appropriate deposition rate law.

2.1. Gas-Phase Model. For the gas-phase model, a vertical, one-dimensional, stagnant flow geometry is considered. The inlet flow consists of two components, hydrogen and silane. Silane diffuses through a stagnant gas film of hydrogen. The temperature is constant throughout the gas phase. Thus, under the assumption of continuum, the silane concentration in the gas phase can be modeled via the following parabolic PDE:

$$\frac{\partial X}{\partial t} = D\frac{\partial^2 X}{\partial z^2} - KX \tag{1}$$

where X is the molar fraction of silane, D is the diffusivity of silane, and the term $-KX$ accounts for the consumption of silane in the gas phase, i.e., via gas-phase reaction and undesired sediments on reactor walls (we assume that this term has a first-order dependence on silane concentration, but other rate laws can be readily used in the present framework).

The diffusivity, D, is calculated using a second order polynomial of temperature as follows:[20]

$$D = c_0 + c_1 T_g + c_2 T_g^2 \tag{2}$$

where T_g is the gas phase temperature set at 300 K, and c_0, c_1, and c_2 are the coefficients of the polynomial whose values are given in Table 1.

The diffusion equation of eq 1 is subject to the initial condition

$$X(z, 0) = 0 \tag{3}$$

the boundary condition at the inlet ($z = z_0 = 0.4$ m)

$$X(z_0, t) = X_{in} \tag{4}$$

where X_{in} is the inlet concentration of silane, and the boundary condition at the wafer surface ($z = 0$)

$$CD\frac{\partial X}{\partial z}(0, t) = R_W \tag{5}$$

where C is the molar concentration of the gas phase right above the surface and R_W is the deposition rate on the wafer surface. Under the assumption of ideal gas, $C = P/(RT_g)$, where P is the gas phase pressure and R is the ideal gas constant.

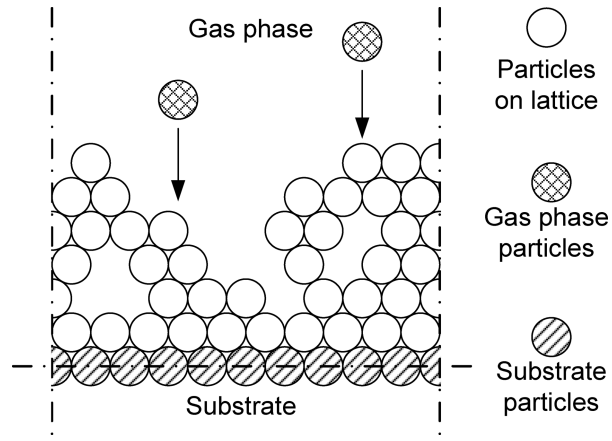

Figure 2. Thin film growth process on a triangular lattice.

When silane diffuses to the wafer surface, it decomposes into silicon and hydrogen as follows:

$$SiH_4 \rightarrow Si + 2H_2 \tag{6}$$

Then, the silicon atoms are deposited onto the thin film. The deposition rate law on the surface is given as follows:[20]

$$R_W = \frac{kPX_s}{1 + K_H(P(1 - X_s))^{1/2} + K_s PX_s} \tag{7}$$

where X_s is the silane concentration at the wafer surface, and k, K_H, and K_s are coefficients in the rate law. The coefficient k follows an Arrhenius-type law as follows:[20]

$$k = 1.6 \times 10^4 \exp(-18500/T_s)\ \text{mol} \cdot \text{m}^{-2} \cdot \text{s}^{-1} \cdot \text{Pa}^{-1} \tag{8}$$

where T_s is the temperature of the wafer surface. The values of the parameters and coefficients of the gas-phase model can be found in Table 1.

2.2. On-lattice Kinetic Monte Carlo Model of Thin Film Growth. The film growth model used in this work is an on-lattice kMC model in which all particles occupy discrete lattice sites.[19,21] The on-lattice kMC model is valid for a low temperature region, $T < 0.5T_m$ (T_m is the melting point of the crystal). A triangular lattice is selected to represent the crystalline structure of the film, as shown in Figure 2. The new particles are always deposited from the top side of the lattice where the gas phase is located. The number of sites in the lateral direction is defined as the lattice size and is denoted by L. In the triangular lattice, a bottom layer in the lattice is initially set to be fully packed and fixed, as shown in Figure 2. There are no vacancies in this layer, and the particles in this layer cannot migrate. This layer acts as the substrate for the deposition and is not counted in the computation of the number of the deposited particles, i.e., this fixed layer does not influence the film microscopic properties. Two types of microscopic processes (Monte Carlo events) are considered: an adsorption process, in which particles are incorporated into the film from the gas phase, and a migration process, in which surface particles move to adjacent sites.[14,16,17,22]

In an adsorption process, an incident particle comes in contact with the film and is incorporated onto the film. The microscopic adsorption rate, W, which is in units of layers per unit time, is equal to the deposition rate, R_W (i.e., $W =$

R_W). The incident particles are initially placed at random positions above the film lattice and move toward the lattice in the vertical direction until contacting the first particle on the film. Upon contact, the particle moves (relaxes) to the nearest vacant site. Surface relaxation is conducted if this site is unstable, i.e., site with only one neighboring particle. When a particle is subject to surface relaxation, the particle moves to its most stable neighboring vacant site and is finally incorporated into the film.

In a migration process, a particle overcomes the energy barrier of the site and jumps to its vacant neighboring site. The migration rate (probability) of a particle follows an Arrhenius-type law with a precalculated activation energy barrier that depends on the local environment of the particle and the substrate temperature. Since the film is thin, the temperature is assumed to be uniform throughout the film. The interior particles (the particles fully surrounded by six nearest neighbors) and the substrate layer particles cannot migrate.

When a particle is subject to migration, it can jump to either of its vacant neighboring sites with equal probability, unless the vacant neighboring site has no nearest neighbors, i.e., the surface particle cannot jump off the film and it can only migrate on the surface. The deposition process is simulated using the continuous-time Monte Carlo (CTMC) method (see ref 18 for details on the microscopic model and simulation algorithm).

2.3. Definitions of Surface Height Profile and Film Site Occupancy Ratio. Utilizing the continuous-time Monte Carlo algorithm, simulations of the kMC model of a porous silicon thin film growth process can be carried out. Snapshots of film microstructure, i.e., the configurations of particles within the triangular lattice, are obtained from the kMC model at various time instants during process evolution. To quantitatively evaluate the thin film microstructure, two variables, surface roughness and film porosity, are introduced in this subsection.

Surface roughness, which measures the texture of the thin film surface, is represented by the root-mean-square (rms) of the surface height profile of the thin film. Determination of surface height profile is slightly different in the triangular lattice model compared to an SOS model. In the SOS model, the surface of the thin film is naturally described by the positions of the top particles of each column. In the triangular lattice model, however, due to the existence of vacancies and overhangs, the definition of the film surface needs further clarification (see ref 21 for details). Specifically, taking into account practical considerations of surface roughness measurements, the surface height profile of a triangular lattice model is defined based on the particles that can be reached in the vertical direction, as shown in Figure 3. In this definition, a particle is considered as a surface particle only if it is not blocked by the particles in the neighboring columns. Therefore, the surface height profile of a porous thin film is the line that connects the sites that are occupied by the surface particles. With this definition, the surface height profile can be treated as a function of the spatial coordinate. Surface roughness, as a measurement of the surface texture, is defined as the standard deviation of the surface height profile from its average height. The mathematical definition of surface roughness is given later in section 3.1.

In addition to film surface roughness, the film site occupancy ratio (SOR) was introduced in ref 18 to represent the extent of the porosity inside the thin film. The mathematical expression of film SOR is defined as follows:

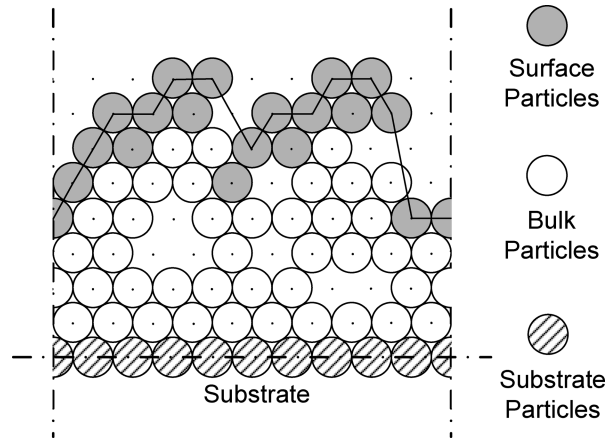

Figure 3. Definition of surface height profile. A surface particle is a particle that is not blocked by particles from both of its neighboring columns in the vertical direction.

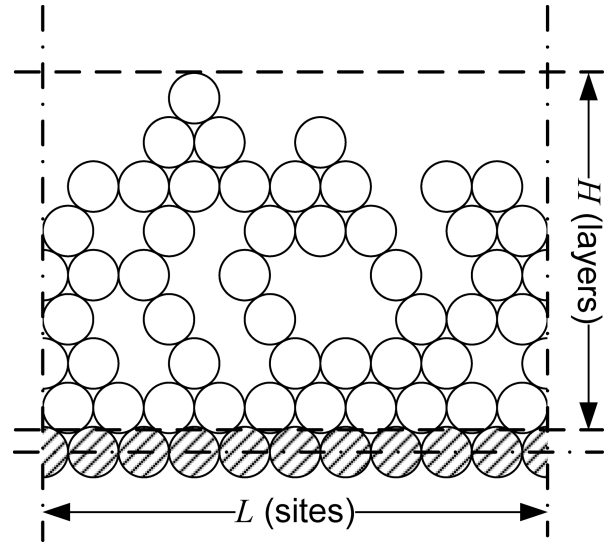

Figure 4. Illustration of the definition of the film SOR of eq 9.

$$\rho = \frac{N}{LH} \tag{9}$$

where ρ denotes the film SOR, N is the total number of deposited particles on the lattice, L is the lattice size, and H denotes the number of deposited layers. Note that the deposited layers are the layers that contain only deposited particles and do not include the initial substrate layers. The variables in the expression of eq 9 can be found in Figure 4. Since each layer contains L sites, the total number of sites in the film that can be contained within the H layers is LH. Thus, film SOR is the ratio of the occupied lattice sites, N, over the total number of available sites, LH. Film SOR ranges from 0 to 1. Specifically, $\rho = 1$ denotes a fully occupied film with a flat surface. The value of zero is assigned to ρ at the beginning of the deposition process since there are no particles deposited on the lattice.

3. Dynamic Model Construction

3.1. Edwards−Wilkinson-type Equation of Surface Height. An Edwards−Wilkinson(EW)-type equation, a second-order stochastic PDE, can be used to describe the surface

height evolution in many microscopic processes that involve thermal balance between adsorption (deposition) and migration (diffusion). Following our previous works,[19,21] an EW-type equation is chosen to describe the dynamics of the fluctuation of surface height (the validation of this choice can be found in ref 23):

$$\frac{\partial h}{\partial t} = r_h + \nu \frac{\partial^2 h}{\partial x^2} + \xi(x,t) \tag{10}$$

subject to periodic boundary conditions

$$h(-\pi,t) = h(\pi,t), \quad \frac{\partial h}{\partial x}(-\pi,t) = \frac{\partial h}{\partial x}(\pi,t) \tag{11}$$

and the initial condition

$$h(x,0) = h_0(x) \tag{12}$$

where $x \in [-\pi,\pi]$ is the spatial coordinate, t is the time, r_h and ν are the model parameters, and $\xi(x,t)$ is a Gaussian white noise with the following mean and covariance:

$$\begin{aligned} \langle \xi(x,t) \rangle &= 0 \\ \langle \xi(x,t)\xi(x',t') \rangle &= \sigma^2 \delta(x-x')\delta(t-t') \end{aligned} \tag{13}$$

where σ^2 is a parameter which measures the intensity of the Gaussian white noise and $\delta(\cdot)$ denotes the standard Dirac delta function. The values of r_h, ν, and σ will be computed so that the solutions of eq 10 approximate well data obtained from the kMC simulations of the thin film growth process.

To proceed with control design, a stochastic ODE approximation of eq 10 is first derived using modal decomposition. Consider the eigenvalue problem of the linear operator of eq 10, which takes the following form:

$$\begin{aligned} A\bar{\phi}_n(x) &= \nu \frac{d^2\bar{\phi}_n(x)}{dx^2} = \lambda_n \bar{\phi}_n(x) \\ \bar{\phi}_n(-\pi) &= \bar{\phi}_n(\pi), \quad \frac{d\bar{\phi}_n}{dx}(-\pi) = \frac{d\bar{\phi}_n}{dx}(\pi) \end{aligned} \tag{14}$$

where λ_n denotes an eigenvalue and $\bar{\phi}_n$ denotes an eigenfunction. A direct computation of the solution of the above eigenvalue problem yields $\lambda_0 = 0$ with $\psi_0 = 1/(2\pi)^{1/2}$, and $\lambda_n = -\nu n^2$ (λ_n is an eigenvalue of multiplicity two) with eigenfunctions $\phi_n = (1/\sqrt{\pi})\sin(nx)$ and $\psi_n = (1/\sqrt{\pi})\cos(nx)$ for $n = 1, ..., \infty$. Note that the $\bar{\phi}_n$ in eq 14 denotes either ϕ_n or ψ_n. The solution of eq 10 is expanded in an infinite series in terms of the eigenfunctions of the operator of eq 14 as follows:

$$h(x,t) = \sum_{n=1}^{\infty} \alpha_n(t)\phi_n(x) + \sum_{n=0}^{\infty} \beta_n(t)\psi_n(x) \tag{15}$$

where $\alpha_n(t)$ and $\beta_n(t)$ are time-varying coefficients. Substituting the above expansion for the solution, $h(x,t)$, into eq 10 and taking the inner product with the adjoint eigenfunctions, $\phi_n^*(x) = (1/\sqrt{\pi})\sin(nx)$ and $\psi_n^*(x) = (1/\sqrt{\pi})\cos(nx)$, the following system of infinite stochastic ODEs is obtained:

$$\begin{aligned} \frac{d\beta_0}{dt} &= \sqrt{2\pi} r_h + \xi_\beta^0(t) \\ \frac{d\alpha_n}{dt} &= \lambda_n \alpha_n + \xi_\alpha^n(t), \quad \frac{d\beta_n}{dt} = \lambda_n \beta_n + \xi_\beta^n(t), \quad n = 1, ..., \infty \end{aligned} \tag{16}$$

where

$$\xi_\alpha^n(t) = \int_{-\pi}^{\pi} \xi(x,t)\phi_n^*(x)\,dx, \quad \xi_\beta^n(t) = \int_{-\pi}^{\pi} \xi(x,t)\psi_n^*(x)\,dx \tag{17}$$

The covariances of $\xi_\alpha^n(t)$ and $\xi_\beta^n(t)$ can be obtained: $\langle \xi_\alpha^n(t)\xi_\alpha^n(t') \rangle = \sigma^2\delta(t-t')$ and $\langle \xi_\beta^n(t)\xi_\beta^n(t') \rangle = \sigma^2\delta(t-t')$. Due to the orthogonality of the eigenfunctions of the operator in the EW equation of eq 10, $\xi_\alpha^n(t)$ and $\xi_\beta^n(t)$, $n = 0,1, ...$, are stochastically independent.

Since the stochastic ODE system is linear, the analytical solution of state variance can be obtained from a direct computation as follows:

$$\begin{aligned} \langle \alpha_n^2(t) \rangle &= \frac{\sigma^2}{2\nu n^2} + \left(\langle \alpha_n^2(t_0) \rangle - \frac{\sigma^2}{2\nu n^2} \right) e^{-2\nu n^2 (t-t_0)} \\ \langle \beta_n^2(t) \rangle &= \frac{\sigma^2}{2\nu n^2} + \left(\langle \beta_n^2(t_0) \rangle - \frac{\sigma^2}{2\nu n^2} \right) e^{-2\nu n^2 (t-t_0)} \\ & n = 1, 2, ..., \infty \end{aligned} \tag{18}$$

where $\langle \alpha_n^2(t_0) \rangle$ and $\langle \beta_n^2(t_0) \rangle$ are the state variances at time t_0. The analytical solution of state variance of eq 18 will be used in the parameter estimation and the MPC design.

When the dynamic model of surface height profile is determined, surface roughness of the thin film is defined as the standard deviation of the surface height profile from its average height and is computed as follows:

$$r(t) = \sqrt{\frac{1}{2\pi} \int_{-\pi}^{\pi} [h(x,t) - \bar{h}(t)]^2\,dx} \tag{19}$$

where $\bar{h}(t) = (1/2\pi)\int_{-\pi}^{\pi} h(x,t)\,dx$ is the average surface height. According to eq 15, we have $\bar{h}(t) = \beta_0(t)\psi_0$. Therefore, $\langle r^2(t) \rangle$ can be rewritten in terms of $\langle \alpha_n^2(t) \rangle$ and $\langle \beta_n^2(t) \rangle$ as follows:

$$\begin{aligned} \langle r^2(t) \rangle &= \frac{1}{2\pi} \left\langle \int_{-\pi}^{\pi} (h(x,t) - \bar{h}(t))^2\,dx \right\rangle \\ &= \frac{1}{2\pi} \left\langle \sum_{i=1}^{\infty} (\alpha_i^2(t) + \beta_i^2(t)) \right\rangle \\ &= \frac{1}{2\pi} \sum_{i=1}^{\infty} [\langle \alpha_i^2(t) \rangle + \langle \beta_i^2(t) \rangle] \end{aligned} \tag{20}$$

where $\bar{h} = (1/2\pi)\int_{-\pi}^{\pi} h(x,t)\,dx = \beta_0(t)\psi_0$ is the average of surface height. Thus, eq 20 provides a direct link between the state variance of the infinite stochastic ODEs of eq 16 and the expected surface roughness of the thin film. However, due to the presence of infinite terms in the summation of eq 20, the solution of the expected surface roughness of eq 20 cannot be directly used in the MPC design. Thus, a reduced-order model is needed and is introduced in the MPC design later in section 4.1. Note that the parameter r_h does not appear in the expression of surface roughness, since only the zeroth state, β_0, is affected by r_h, but this state is not included in the computation of the expected surface roughness square of eq 20.

Film thickness, which is represented by the average of surface height, $\bar{h}$, is another objective under consideration in this work. The dynamics of the expected value of averaged surface height can be obtained from the analytical solution of the zeroth state, β_0, from eq 16, as follows:

$$\frac{d\langle \bar{h} \rangle}{dt} = r_h \tag{21}$$

The analytical solution of expected value of film thickness, $\langle \bar{h} \rangle$, can be obtained directly from eq 21 as follows:

$$\langle \bar{h}(t) \rangle = \langle \bar{h}(t_0) \rangle + r_h(t - t_0) \tag{22}$$

3.2. Dynamic Model of Film Site Occupancy Ratio. The concept of film site occupancy ratio (SOR) is used to characterize film porosity. According to the definition of film SOR of eq 9, film SOR accounts for all deposited layers during the entire deposition process. Thus, film SOR is a cumulative property, the evolution of which can be characterized by an integral form. Before further derivation of the dynamic model of film SOR, a concept of instantaneous film SOR of the film layers deposited between time t and $t + dt$, denoted by ρ_d, is first introduced as the spatial derivative of the number of deposited particles in the growing direction as follows:

$$\rho_d = \frac{dN}{d(HL)} \tag{23}$$

In eq 23, the lattice size L is a constant and the derivative dH can be written as a linear function of time derivative dt as follows:

$$dH = r_H \, dt \tag{24}$$

where r_H is the growth rate of the thin film from the top layer point of view. Note that r_H is different from the model coefficient r_h in eq 10. Thus, the expressions of N and H can be obtained by integrating eqs 23 and 24 as follows:

$$\begin{aligned} N(t) &= L \int_0^t \rho_d r_H \, ds \\ H(t) &= \int_0^t r_H \, ds \end{aligned} \tag{25}$$

With the definition of ρ of eq 9 and the expressions of N and H of eq 25, the film SOR of eq 9 can be rewritten in an integral form as follows:

$$\rho = \frac{\int_0^t \rho_d r_H \, ds}{\int_0^t r_H \, ds} \tag{26}$$

To simplify the subsequent development and develop an SOR model that is suitable for control purposes, we assume (this assumption will be verified in the closed-loop simulation results below where the performance of the controller will be evaluated) that the dynamics of the instantaneous film SOR, ρ_d, can be approximated by a linear first-order process, i.e.:

$$\tau \frac{d\rho_d(t)}{dt} = \rho_d^{ss} - \rho_d(t) \tag{27}$$

where τ is the time constant and ρ_d^{ss} is the steady-state value of the instantaneous film SOR. We note that the first-order ODE model of eq 27 was introduced and justified with numerical results in refs 18 and 23 for the modeling of the partial film SOR, which is defined to characterize the evolution of the film porosity of layers that are close to the film surface. In this work, the instantaneous film SOR is a similar concept to the partial film SOR, because it also describes the contribution to the bulk film porosity of the newly deposited layers. Therefore, the first-order ODE model is a suitable choice to describe the evolution of the instantaneous film SOR.

From eq 26, it follows that at large times as ρ_d approaches ρ_d^{ss}, the steady-state film SOR (ρ^{ss}) approaches the steady-state value of the instantaneous film SOR (i.e., $\rho^{ss} = \rho_d^{ss}$). The deterministic ODE system of eq 27 is subject to the following initial condition:

$$\rho_d(t_0) = \rho_{d0} \tag{28}$$

where t_0 is the initial time and ρ_{d0} is the initial value of the instantaneous film SOR. From eqs 27 and 28 and the fact that $\rho^{ss} = \rho_d^{ss}$ at large times, it follows that

$$\rho_d(t) = \rho^{ss} + (\rho_{d0} - \rho^{ss}) e^{-(t-t_0)/\tau} \tag{29}$$

For controller implementation purposes, the expression of the film SOR can be derived as follows:

$$\begin{aligned} \rho(t) &= \frac{\int_0^{t_0} \rho_d r_H \, ds + \int_{t_0}^t \rho_d r_H \, ds}{\int_0^{t_0} r_H \, ds + \int_{t_0}^t r_H \, ds} \\ &= \frac{\rho_0 H_0 + \int_{t_0}^t \rho_d r_H \, ds}{H_0 + \int_{t_0}^t r_H \, ds} \end{aligned} \tag{30}$$

where t_0 is the current time, ρ_0 and H_0 are film SOR and film height at time t_0, respectively.

Substituting the solution of ρ_d of eq 29 into eq 30 and assuming that r_H is constant for $t > \tau > t_0$, which is taken to be the case in the parameter estimation and the MPC formulations below, the analytical solution of film SOR at time t can be obtained as follows:

$$\rho = \frac{\rho_0 H_0 + r_H[\rho^{ss}(t - t_0) + (\rho^{ss} - \rho_0)\tau(e^{-(t-t_0)/\tau} - 1)]}{H_0 + r_H(t - t_0)} \tag{31}$$

which is directly utilized in the model predictive control formulation of eq 34 below.

4. Model Predictive Controller Design

In this section, model predictive controllers are designed to regulate the expected values of film roughness square, SOR, and thickness to desired levels by manipulating the inlet silane concentration. Two different ways of implementing the desired film thickness requirement are presented and compared. A reduced-order model of the EW equation is used in the MPC formulation to approximate the dynamics of the surface roughness. State feedback control is considered in this section to present the control algorithms, i.e., the surface height profile and the value of film SOR are assumed to be available to the controller. Porosity estimation-based model predictive control is considered in section 6.

4.1. Reduced-Order Model for Surface Roughness. In the MPC formulation, the expected surface roughness may be computed from the EW equation of eq 10 by substituting the solution of the state variance of eq 18 into the expression of the expected surface roughness square of eq 20. However, the EW equation is a distributed parameter dynamic model, which contains infinite dimensional stochastic states. Therefore, the solution of the EW equation leads to a model predictive controller of infinite order that cannot be realized

in practice (i.e., the practical implementation of a control algorithm based on such a system will require the computation of infinite sums which cannot be done by a computer). To this end, a reduced-order model of the infinite dimensional ODE model of eq 16 is instead derived and used to calculate the prediction of the expected surface roughness in the model predictive controller.

Due to the structure of the eigenspectrum of the linear operator of the EW equation of eq 10, the dynamics of the EW equation are characterized by a finite number of dominant modes. By neglecting the high-order modes ($n \geq m + 1$), the system of eq 16 can be approximated by a finite-dimensional system as follows:

$$\frac{d\alpha_n}{dt} = \lambda_n \alpha_n + \xi_\alpha{}^n(t), \quad \frac{d\beta_n}{dt} = \lambda_n \beta_n + \xi_\beta{}^n(t) \qquad n = 1, ..., m \tag{32}$$

Note that the ODE for the zeroth state is also neglected, since the zeroth state does not contribute to surface roughness.

Using the finite-dimensional system of eq 32, the expected surface roughness square, $\langle r^2(t)\rangle$, can be approximated with the finite-dimensional state variance as follows:

$$\langle \tilde{r}^2(t)\rangle = \frac{1}{2\pi}\sum_{i=1}^{m}[\langle \alpha_i{}^2(t)\rangle + \langle \beta_i{}^2(t)\rangle] \tag{33}$$

where the tilde symbol in $\langle \tilde{r}^2(t)\rangle$ denotes its association with a finite-dimensional system.

4.2. MPC Formulation. We consider the control problem of film surface roughness, porosity, and thickness regulation by using a model predictive control design. The expected values, $\langle r^2\rangle$, $\langle \rho\rangle$, and $\langle \bar{h}\rangle$, are chosen as the control objectives. The adsorption rate is computed by the controller, which, in turn, is used to calculate the inlet silane concentration via eq 7 (i.e., the presence of the gas phase is neglected in the calculation of the control action, X_{in}, but it is accounted for in the multiscale process model, where the control action is applied). The substrate temperature is fixed at 850 K during the entire closed-loop simulation. The control action is obtained by solving a finite-horizon optimal control problem.

The cost function in the optimal control problem (eq 34 below) includes penalty on the deviation of $\langle r^2\rangle$ and $\langle \rho\rangle$ from their respective set-point values. However, since the manipulated input variable is the adsorption rate and the film deposition process is a batch operation (i.e., the film growth process is terminated within a certain time), a desired value of the film thickness is also required to prevent an undergrown thin film at the end of the deposition process. Therefore, in the MPC shown in eq 34, the desired film thickness is regarded as the set-point value of the film thickness, i.e., the deviation of the film thickness from the desired value is included in the cost function. However, only the negative deviation (when the film thickness is less than the desired value) is penalized; no penalty is imposed on the deviation when the thin film thickness exceeds the desired thickness. Different weighting factors are assigned to the penalties on the deviations of the expected values of film surface roughness, SOR, and thickness from their desired values. Relative deviations are used in the formulation of the cost function to make the magnitude of the different terms comparable. The optimization problem is subject to the dynamics of the reduced-order model of surface roughness of eq 32, the dynamics of the film thickness of eq 21, and the dynamics of the film SOR of eq 26. The optimal profile of the adsorption rate is calculated by solving a finite-dimensional optimization problem in a receding horizon fashion. Specifically, the MPC problem is formulated as follows:

$$\begin{aligned}
&\min_{W_1,...,W_i,...,W_p} J = \sum_{i=1}^{p}\{q_{r^2,i}F_{r^2,i} + q_{h,i}F_{h,i} + q_{\rho,i}F_{\rho,i}\}\\
&\text{subject to}\\
&F_{r^2,i} = \left[\frac{r_{set}{}^2 - \langle \tilde{r}^2(t_i)\rangle}{r_{set}{}^2}\right]^2\\
&F_{h,i} = \begin{cases}\left[\dfrac{h_{min} - \langle \bar{h}(t_i)\rangle}{h_{min}}\right]^2, & h_{min} > \langle \bar{h}(t_i)\rangle\\ 0, & h_{min} \leq \langle \bar{h}(t_i)\rangle\end{cases}\\
&F_{\rho,i} = \left[\frac{\rho_{set} - \langle \rho(t_i)\rangle}{\rho_{set}}\right]^2\\
&\langle \alpha_n{}^2(t_i)\rangle = \frac{\sigma^2}{2\nu n^2} + \left(\langle \alpha_n{}^2(t_{i-1})\rangle - \frac{\sigma^2}{2\nu n^2}\right)e^{-2\nu n^2\Delta}\\
&\langle \beta_n{}^2(t_i)\rangle = \frac{\sigma^2}{2\nu n^2} + \left(\langle \beta_n{}^2(t_{i-1})\rangle - \frac{\sigma^2}{2\nu n^2}\right)e^{-2\nu n^2\Delta}\\
&\langle \bar{h}(t_i)\rangle = \langle \bar{h}(t_{i-1})\rangle + r_h\Delta\\
&\langle \rho(t_i)\rangle = \frac{1}{\langle \bar{h}(t_{i-1})\rangle + r_h\Delta}\{\langle \rho(t_{i-1})\rangle\langle \bar{h}(t_{i-1})\rangle +\\
&\qquad r_h[\rho^{ss}\Delta + (\rho^{ss} - \langle \rho(t_{i-1})\rangle)\tau_p(e^{-\Delta/\tau_p} - 1)]\}\\
&W_{min} < W_i < W_{max}, \quad i = 1, 2, ..., p
\end{aligned} \tag{34}$$

where t is the current time, Δ is the sampling time, p is the number of prediction steps, $p\Delta$ is the specified prediction horizon, t_i, $i = 1, 2, ..., p$, is the time of the ith prediction step ($t_i = t + i\Delta$), respectively, W_i, $i = 1, 2, ..., p$, is the adsorption rate at the ith step ($W_i = W(t + i\Delta)$), respectively, $q_{r^2,i}$, $q_{h,i}$, and $q_{\rho,i}$, $i = 1, 2, ..., p$, are the weighting penalty factors for the deviations of $\langle r^2\rangle$ and $\langle \rho\rangle$ from their respective setpoints r_{set}^2 and ρ_{set}, $\langle \bar{h}\rangle$ from its desired h_{min}, at the ith prediction step, and W_{min} and W_{max} are the lower and upper bounds on the deposition rate, respectively. Note that we choose $\langle \bar{h}\rangle$, r_h, and $\rho(t_0)$ to replace H, r_H, and ρ_{d0} in the MPC formulation of eq 34, respectively.

The optimal set of (W_1, W_2, ..., W_p), is obtained from the solution of the multivariable optimization problem of eq 34, and only the first value of the manipulated input trajectory, W_1, is used to compute the inlet silane concentration and is applied to the deposition process from time t until the next sampling time, when new measurements are received and the MPC problem of eq 34 is solved for the computation of the next optimal input trajectory.

The dependence of the model coefficients, r_h, ν, σ^2, ρ^{ss}, and τ, on adsorption rate is used in the formulation of the model predictive controller of eq 34. Thus, parameter estimation from open-loop kMC simulation results of the thin film growth process for a variety of operation conditions is performed to obtain the dependence of the model coefficients on adsorption rate using least-squares methods.[21]

Remark 1. *In the MPC formulation shown in eq 34, the desired thickness requirement is implemented by including penalty on the negative deviation of the expected film thickness from its set point in the cost function. This formulation cannot guarantee that the final film thickness is greater than the set-point value, thus it can be viewed as a soft constraint*

formulation. To ensure that the thickness requirement would be satisfied, a thickness constraint should be implemented as a lower bound on deposition rate, which is the smallest deposition rate needed to reach the desired thickness at the end of the deposition process. The modified MPC, accounting for the gas phase via a constant gain, can be then formulated as follows:

$$\min_{W_1,\ldots,W_i,\ldots,W_p} J = \sum_{i=1}^{p} \{q_{r^2,i}F_{r^2,i} + q_{\rho,i}F_{\rho,i}\}$$

subject to

$$F_{r^2,i} = \left[\frac{r_{\text{set}}^{\,2} - \langle \tilde{r}^2(t_i)\rangle}{r_{\text{set}}^{\,2}}\right]^2$$

$$F_{\rho,i} = \left[\frac{\rho_{\text{set}} - \langle \rho(t_i)\rangle}{\rho_{\text{set}}}\right]^2$$

$$\langle \alpha_n^{\,2}(t_i)\rangle = \frac{\sigma^2}{2\nu n^2} + \left(\langle \alpha_n^{\,2}(t_{i-1})\rangle - \frac{\sigma^2}{2\nu n^2}\right)e^{-2\nu n^2\Delta}$$

$$\langle \beta_n^{\,2}(t_i)\rangle = \frac{\sigma^2}{2\nu n^2} + \left(\langle \beta_n^{\,2}(t_{i-1})\rangle - \frac{\sigma^2}{2\nu n^2}\right)e^{-2\nu n^2\Delta}$$

$$\langle \bar{h}(t_i)\rangle = \langle \bar{h}(t_{i-1})\rangle + r_h\Delta$$

$$\langle \rho(t_i)\rangle = \frac{1}{\langle \bar{h}(t_{i-1})\rangle + r_h\Delta}\{\langle \rho(t_{i-1})\rangle\langle \bar{h}(t_{i-1})\rangle + r_h[\rho^{ss}\Delta + (\rho^{ss} - \langle \rho(t_{i-1})\rangle)\tau_p(e^{-\Delta/\tau_p} - 1)]\}$$

$$W_{\min} < W_i < W_{\max}, \quad i = 1, 2, \ldots, p$$

$$r_h > \frac{h_{\min} - h(t_i)}{(t_{\text{end}} - t_i)}, \quad i = 1, 2, \ldots, p \qquad (35)$$

It is important to note that it is possible that the required minimum deposition rate is larger than the upper bound imposed on W, thereby resulting in an infeasible optimization problem. If this happens, the lower bound is reset to W_{max}-0.001.

Remark 2. *A multivariable control algorithm can be developed for more improved closed-loop control by simultaneously manipulating two or more process input variables. For example, the adsorption rate, W, and the substrate temperature, T, may be used as two simultaneous manipulated inputs in a multivariable control design. The MPC framework presented in this work is suitable for multivariable control system design. However, parameter estimation for a wider range of operating conditions is required to capture the parameter dependence on the adsorption rate and the substrate temperature. Such a parameter dependence may be tabulated via interpolation or formulated via linear or nonlinear regression.*[10]

Remark 3. *Another possible improvement for the control of a thin film growth process is to take into account the transition and crossover of the thin film growth behavior. Specifically, we have recently found*[23] *that at different regions of operating conditions, i.e., adsorption rate and substrate temperature, the growth behavior of thin films may be described by different dynamic models. At low temperatures, the surface profile of a porous thin film follows closely the EW dynamics. As temperature increases, the growth behavior deviates from the EW equation. Other dynamic models (Kardar−Parisi−Zhang-type equations or the stochastic Kuramoto−Sivashinsky equation) may be more suitable to describe the evolution of the thin film surface profile. Therefore, the transition and crossover may be incorporated into the control design by switching the dynamic models at different regions of operation conditions. While the control system designed in this work is successful in achieving the control objectives, the use of even more accurate dynamic models of the film growth at different regimes may help further improve the accuracy of predictions in the MPC.*

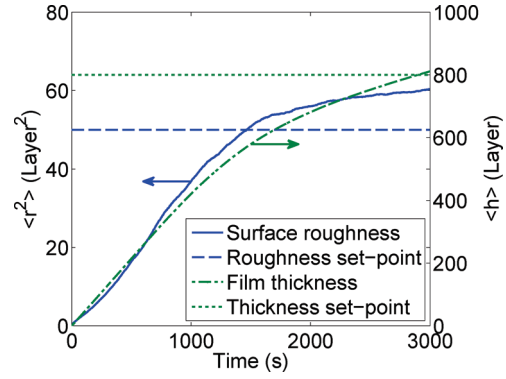

Figure 5. Profiles of the expected values of surface roughness square (solid line, left *y*-axis) and of film thickness (dashed−dotted line, right *y*-axis) under closed-loop operation using the MPC formulation of eq 34 with $q_{r^2,i} = 0.1$, $q_{h,i} = 1$, and $q_{\rho,i} = 0$.

5. Simulation Results

In this section, the proposed model predictive controllers of eqs 34 and 35 are applied to the multiscale model of the thin film growth process described in section 2. The value of the adsorption rate is obtained from the solution of the optimization problem at each sampling time. The corresponding inlet concentration of silane is calculated from the adsorption rate based on the rate law of eq 7 and is applied to the closed-loop system until the next sampling time. The optimization problems in the MPC formulations of eqs 34 and 35 are solved via a local constrained minimization algorithm using a broad set of initial guesses.

The desired values (set-point values) in the closed-loop simulations are $r_{\text{set}}^{\,2} = 50$ layer^2 and $\rho_{\text{set}} = 0.985$, with a desired film thickness of $h_{\min} = 800$ layers. The substrate temperature is fixed at 850 K. The variation of adsorption rate is from 0.1 to 0.45 layer/s (0.45 layer/s is the maximum adsorption rate that can be obtained according to the rate law of eq 7 at $X_s = 1$ and the given conditions of the gas phase in Table 1). The number of prediction steps is set to be $p = 5$. The prediction horizon of each step is fixed at $\Delta = 5$ s. The closed-loop simulation duration is 3000 s. All expected values are obtained from 1000 independent simulation runs.

5.1. Regulation of Film Surface Roughness and Thickness. Closed-loop simulations of regulating film surface roughness and thickness are first carried out. In these control problems, the control objective is to regulate the expected surface roughness square and expected film thickness to desired values. Thus, the cost functions of these problems contain penalties on the deviations of the expected surface roughness square from the set-point value and of the expected film thickness from the desired value. The weighting factors are $q_{r^2,i} = 0.1$, $q_{h,i} = 1$ and $q_{\rho,i} = 0$ for all i.

Figure 5 shows the closed-loop simulation results of the roughness-thickness control problem. From Figure 5, it can be seen that the model predictive controller drives the expected film thickness close to the desired value, at the end of the simulation. However, due to the requirement of achieving a desired film thickness value, which includes a higher penalty factor, the controller computes a higher adsorption rate, and thus, it results in a higher expected surface roughness square at the end of the closed-loop simulation. The effect of the penalty

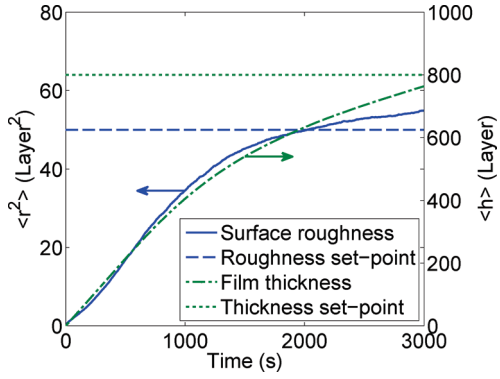

Figure 6. Profiles of the expected values of surface roughness square (solid line, left y-axis) and of film thickness (dashed−dotted line, right y-axis) under closed-loop operation using the MPC formulation of eq 34 with $q_{r^2},i = 1$, $q_{h,i} = 0$, and $q_{\rho,i} = 0$.

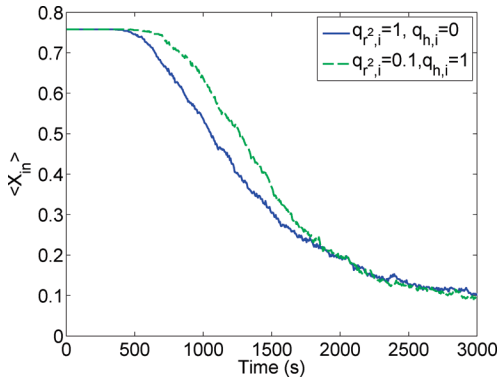

Figure 7. Profiles of expected inlet silane concentrations under closed-loop operation using the MPC formulation of eq 34 with $q_{r^2},i = 0.1$, $q_{h,i} = 1$, and $q_{\rho,i} = 0$ and the MPC formulation of eq 34 with $q_{r^2},i = 1$, $q_{h,i} = 0$, and $q_{\rho,i} = 0$ (dashed line).

on film thickness can be observed by comparing Figure 5 to Figure 6, which shows the closed-loop simulation results without penalty on film thickness. It can be clearly seen that, without penalty on the deviation of film thickness from its desired value, the expected surface roughness square approaches closer to the set-point value at the end of the simulation, while the expected film thickness is lower than the desired value. Figure 7 shows the corresponding profiles of the mean value of inlet precursor concentration for both cases, which demonstrates that in the simulation runs of Figure 5 (where a higher penalty is used on film thickness) the controller uses a higher deposition rate. Figure 8 shows the histogram of film thickness from 1000 independent simulation runs at the end of the simulations ($t =$ 3000 s) using the MPC formulation of eq 34 with $q_{r^2},i = 0.1$, $q_{h,i} = 1$, and $q_{\rho,i} = 0$. Although the mean value is around 800, the distribution is wide and there are many simulations in which the thickness set-point is not reached. The histogram of roughness square is shown in Figure 9. In this case, the mean value is 60.37.

5.2. Regulation of Film Porosity. In this subsection, it is demonstrated that the precise regulation of SOR to its set point can be achieved. Figure 10 shows the closed-loop simulation results of the porosity control problem where the cost function includes only a penalty on the deviation of film SOR from the desired value, 0.985. The histogram of SOR is also presented in Figure 11, and the mean value is 0.9845. We conclude from these two figures that the model predictive controller successfully drives the expected film SOR to the set-point value.

5.3. Simultaneous Regulation of Film Surface Roughness, Porosity, and Thickness. Closed-loop simulations of simultaneous regulation of film thickness, surface roughness, and SOR are carried out with the same weighting factors. Since the inlet silane concentration is the only manipulated input, the desired values of r_{set}^2 and ρ_{set} cannot be achieved simultaneously, i.e., the values of inlet silane concentration needed to achieve the desired surface roughness and film thickness are not the same. Therefore, a trade-off between the two set-points is made by the controller. Figures 12 and 13 show the simulation results for this scenario. The expected values of both surface roughness square and film SOR approach their corresponding set-points and the expected film

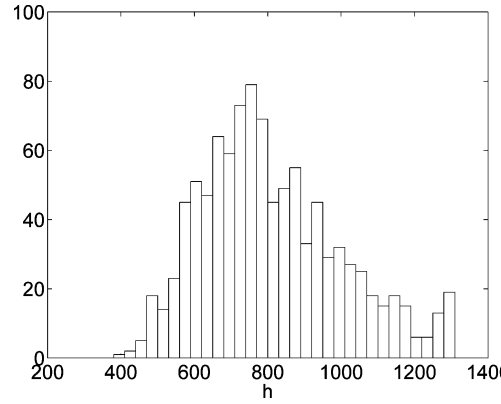

Figure 8. Histogram of closed-loop film thickness at the end of simulation ($t = 3000$ s) using the MPC formulation of eq 34 with $q_{r^2},i = 0.1$, $q_{h,i} = 1$, and $q_{\rho,i} = 0$.

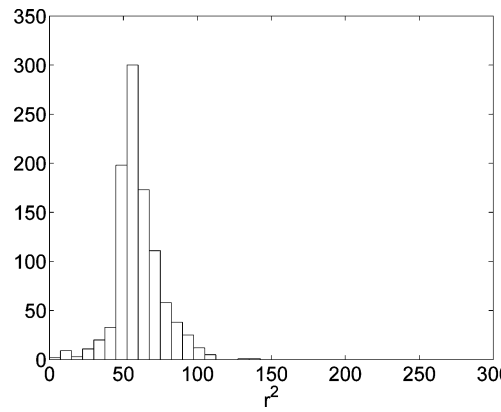

Figure 9. Histogram of closed-loop surface roughness square at the end of simulation ($t = 3000$ s) using the MPC formulation of eq 34 with $q_{r^2},i = 0.1$, $q_{h,i} = 1$, and $q_{\rho,i} = 0$.

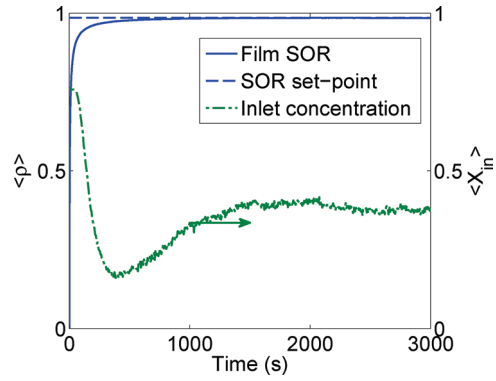

Figure 10. Profiles of the expected values of film SOR (solid line, left y-axis) and of inlet silane concentration (dashed−dotted line, right y-axis) under closed-loop operation using the MPC formulation of eq 34 with $q_{r^2},i = 0$, $q_{h,i} = 0$, and $q_{\rho,i} = 1$.

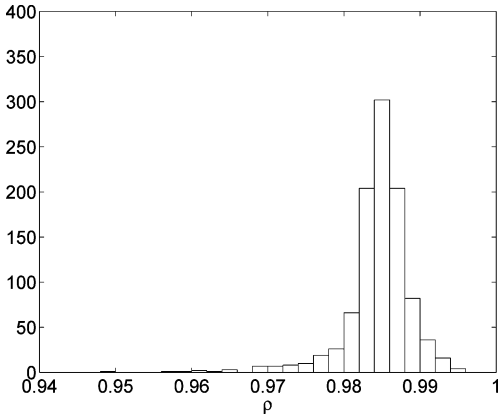

Figure 11. Histogram of closed-loop SOR at the end of simulation (t = 3000 s) using the MPC formulation of eq 34 with $q_{r^2},i = 0$, $q_{h,i} = 0$, and $q_{\rho,i} = 1$.

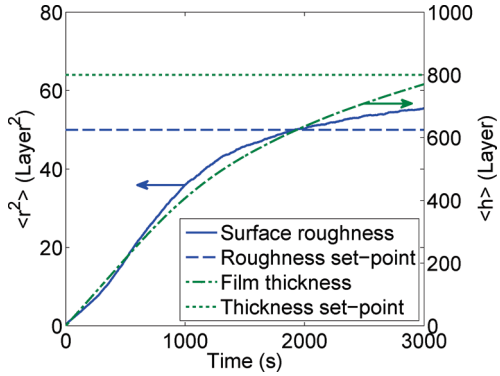

Figure 12. Profiles of the expected values of surface roughness square (solid line, left y-axis) and of film thickness (dashed−dotted line, right y-axis) under closed-loop operation using the MPC formulation of eq 34 with $q_{r^2},i = 1$, $q_{h,i} = 1$, and $q_{\rho,i} = 1$.

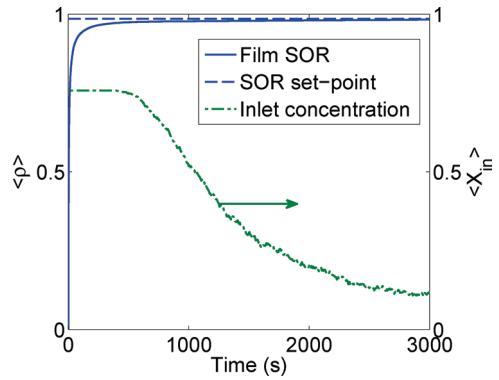

Figure 13. Profiles of the expected values of film SOR (solid line, left y-axis) and of inlet silane concentration (dashed−dotted line, right y-axis) under closed-loop operation using the MPC formulation of eq 34 with $q_{r^2},i = 1$, $q_{h,i} = 1$, and $q_{\rho,i} = 1$.

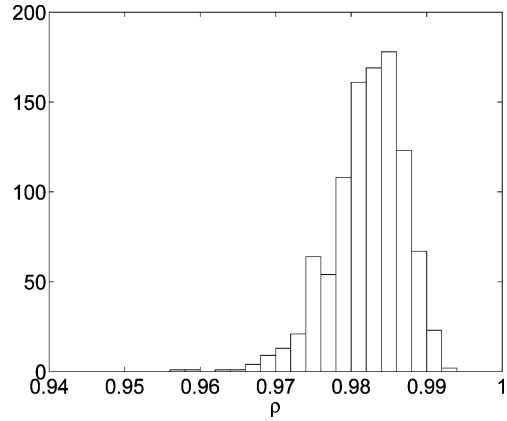

Figure 14. Histogram of closed-loop SOR at the end of simulation (t = 3000 s) using the MPC formulation of eq 34 with $q_{r^2},i = 1$, $q_{h,i} = 1$, and $q_{\rho,i} = 1$.

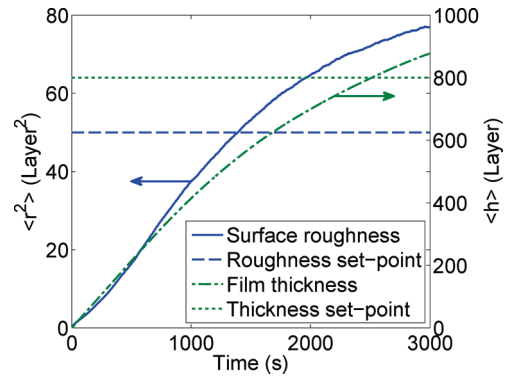

Figure 15. Profiles of the expected values of surface roughness square (solid line, left y-axis) and of film thickness (dashed−dotted line, right y-axis) under closed-loop operation using the MPC formulation of eq 35 with $q_{r^2},i = 0.1$, $q_{h,i} = 0$, and $q_{\rho,i} = 0$.

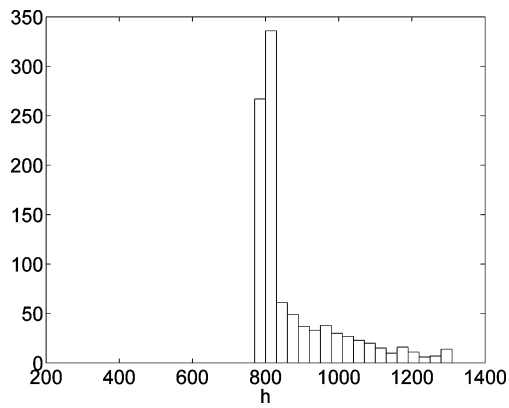

Figure 16. Histogram of closed-loop film thickness at the end of simulation (t = 3000 s) using the MPC formulation of eq 35 with $q_{r^2},i = 0.1$, $q_{h,i} = 0$, and $q_{\rho,i} = 0$.

thickness is lower than the desired one. Figure 14 shows the histogram of SOR, where a very narrow distribution around the mean value is observed.

5.4. Regulation of Roughness with a Constraint on Film Thickness. In this subsection, the modified model predictive controller of eq 35 is applied to the regulation of surface roughness and film thickness. The cost function penalizes only roughness deviation, and the weighting factors are $q_{r^2},i = 0.1$ and $q_{\rho,i} = q_{h,i} = 0$.

Figure 15 shows the profile of the mean value of thickness and roughness. The MPC drives the thickness above the desired minimum value. The offset of the roughness square at the end of simulation is larger compared to the result shown in Figure 5 where the film thickness is penalized in the cost function. Figure 16 shows the histogram of film thickness for 1000 simulation runs. Almost every run reaches the minimum thickness requirement, and the maximum negative offset is less than 1. This can be compared with the result of the MPC formulation of eq 34, where about 50% of the simulation runs do not satisfy the thickness requirement. Figure 17 shows the histograms of roughness square. Its distribution is wider compared with the result of MPC of eq 34, shown in Figure 9.

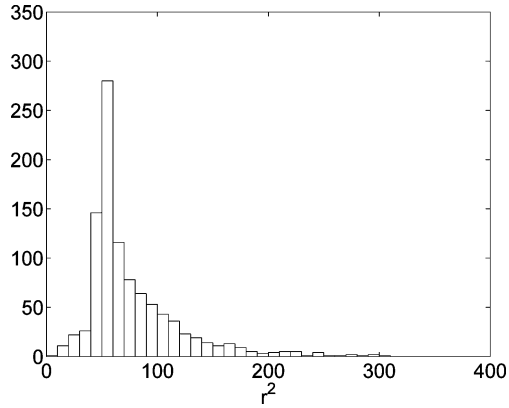

Figure 17. Histogram of closed-loop surface roughness square at the end of simulation ($t = 3000$ s) using the MPC formulation of eq 35 with $q_{r^2,i} = 0.1$, $q_{h,i} = 0$, and $q_{\rho,i} = 0$.

It should be pointed out that the relative weighting between thickness and roughness deviation plays a key role in the MPC of eq 34. For example, by increasing the relative weighting of thickness over roughness from 10 to 1000, the mean value of the film thickness can be larger than the set point at the expense of a much higher surface roughness.

6. Porosity Estimation-Based Model Predictive Control

The MPC formulations of eqs 34 and 35 have been derived under the state feedback assumption. In this assumption, all the required information about the thin film state can be measured in real time during the closed-loop operation. However, it may be difficult to measure the film porosity online with currently available techniques, and thus, state feedback control of film SOR may not be possible to be directly implemented in practice. To address this problem, an estimation scheme is needed to estimate the film porosity from other available film measurements, e.g., the surface profile of the thin film. The proposed MPC formulations will then use the estimates of the film SOR in the optimization problem to compute the optimal solution for the manipulated input.

To estimate the film porosity, we need the following assumptions:

1. The number of deposited layers, H, is available or can be measured from the surface profile of the thin film.

2. The adsorption rate at the wafer surface, W, can be obtained, either from the simulation of the gas phase model or by measuring the surface precursor concentration.

By substituting the number of deposited particles, N, with the integral of the adsorption rate for the entire deposition duration in the definition of film SOR of eq 9, film SOR can be estimated by the following equation:

$$\hat{\rho}(t_i) = \frac{\int_0^{t_i} W(t_i)\,\mathrm{d}t}{H(t_i)} \approx \frac{\hat{\rho}(t_{i-1})H(t_{i-1}) + \sum_1^i W(t_i)\Delta}{H(t_i)} \quad (36)$$

where $\hat{\rho}(t_i)$ is the estimated film SOR.

To compare the estimated film SOR with its actual value computed by the multiscale process model, we plot the profiles of the estimated and of the actual SOR value from a single simulation run in Figure 18. It can been seen that the estimate follows closely the actual film SOR but reaches a lower steady-state value at large times.

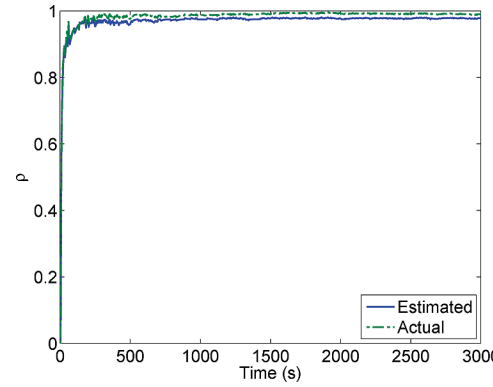

Figure 18. Profiles of SOR estimated via eq 36 (solid line) and computed directly from the multiscale process model (dashed−dotted line).

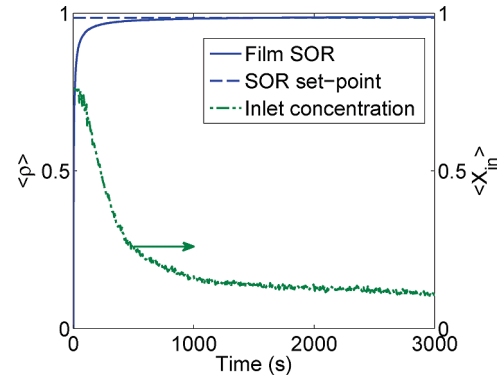

Figure 19. Profiles of the expected value of film SOR (solid line, left y-axis) and of inlet silane concentration (dashed−dotted line, right y-axis) under closed-loop operation using the MPC formulation of eq 34 with $q_{r^2,i} = 0$, $q_{h,i} = 0$, and $q_\rho = 1$ and porosity estimation.

Using the estimation scheme of film SOR of eq 36, we can construct an output feedback controller by combining the MPC formulations of eqs 34 or 35 and the estimation scheme. To demonstrate the effectiveness of the estimation scheme and of the output feedback controller, we first consider the porosity-only control problem. The MPC formulation of eq 34 is used in the output feedback controller. The same operating conditions are used in the output feedback control problem as in the state feedback control problem in section 5. Figure 19 shows the profiles of the film SOR and of the inlet concentration of silane. The output feedback controller successfully stabilizes the porosity close to the set point value, 0.985. Figure 20 shows the histogram of SOR at $t = 3000$ s under the output feedback controller. It can be clearly seen that the output feedback controller results in a wider distribution of film SOR at the end of the simulation compared to the one under state feedback control, which is expected due to the error introduced by porosity estimation.

To further demonstrate the applicability of the output feedback controller, we also consider simultaneous output feedback control of film surface roughness, porosity and thickness. The closed-loop simulation results can be found in Figures 21 and 22, which show the profiles of the expected value of the film thickness, roughness square, film SOR, and of the inlet silane concentration, respectively. The closed-loop profiles under output feedback control are close to the results under state feedback control presented in section 5.3, which is reasonable since the film porosity is estimated quite well. The histogram of the film SOR is also shown in Figure 23; it has a wider spread compared to the one under state feedback control (Figure 14) owing to the error introduced by the estimation.

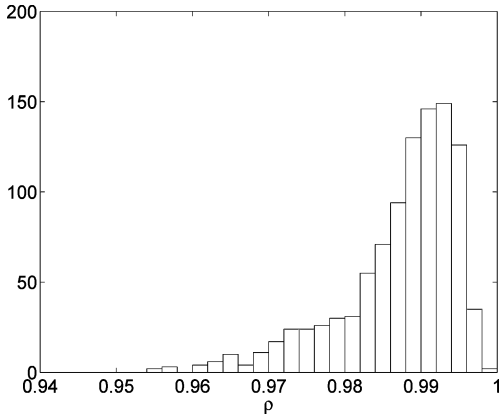

Figure 20. Histogram of closed-loop SOR at the end of simulation (t = 3000 s) using the MPC formulation of eq 34 with $q_{r^2},i = 0$, $q_{h,i} = 0$, and $q_\rho = 1$ and porosity estimation.

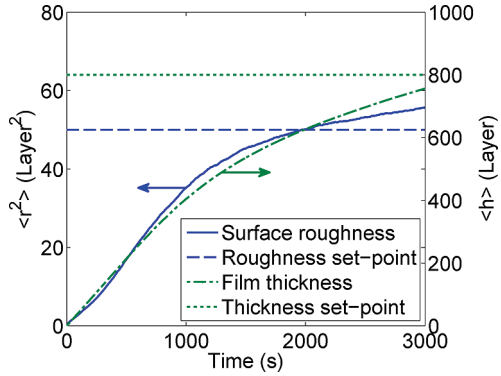

Figure 21. Profiles of the expected values of film SOR (solid line, left y-axis) and of inlet silane concentration (dashed−dotted line, right y-axis) under closed-loop operation using the MPC formulation of eq 34 with $q_{r^2},i = 1$, $q_{h,i} = 1$, and $q_\rho = 1$ and porosity estimation.

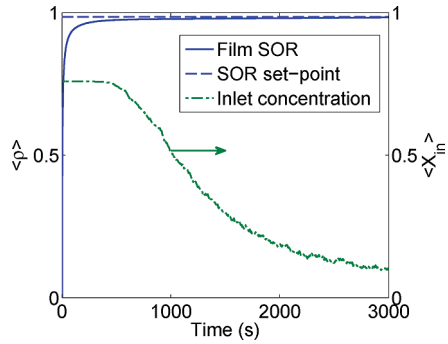

Figure 22. Profiles of the expected values of film SOR (solid line, left y-axis) and of inlet silane concentration (dashed−dotted line, right y-axis) under closed-loop operation using the MPC formulation of eq 34 with $q_{r^2},i = 1$, $q_{h,i} = 1$, and $q_\rho = 1$ and porosity estimation.

7. Conclusions

In this work, we developed model predictive control algorithms to simultaneously control film surface roughness, porosity, and thickness in a multiscale model of a thin film growth process. On the macroscopic side, the gas phase dynamics was modeled by a continuous PDE model derived from a mass balance. On the microscopic side, the thin film deposition process was simulated via a kinetic Monte Carlo model developed on a triangular lattice with vacancies and overhangs allowed inside the film. Dynamic models of film surface height

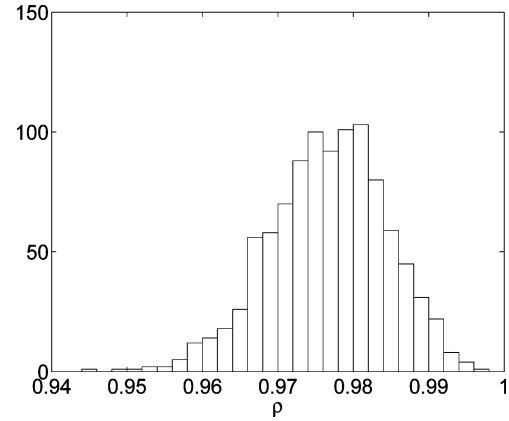

Figure 23. Histogram of closed-loop SOR at the end of simulation (t = 3000 s) using the MPC formulation of eq 34 with $q_{r^2},i = 1$, $q_{h,i} = 1$, and $q_\rho = 1$ and porosity estimation.

and film porosity were developed and used in the MPC algorithms. The regulation of film thickness was addressed in two different ways. One way is to include penalty on the deviation of the film thickness into the cost function, and the other one is to impose a constraint on the adsorption rate to ensure the desired film thickness at the end of the film growth process. The proposed model predictive controllers were applied to the multiscale thin film growth model to evaluate their performance. In addition, an estimation scheme of film SOR was introduced and used successfully in conjunction with the MPC schemes.

Acknowledgment

Financial support from NSF, CBET-0652131, is gratefully acknowledged.

Literature Cited

(1) Lou, Y.; Christofides, P. D. Estimation and Control of Surface Roughness in Thin Film Growth Using Kinetic Monte-Carlo Models. *Chem. Eng. Sci.* **2003**, *58*, 3115–3129.

(2) Christofides, P. D.; Armaou, A.; Lou, Y.; Varshney, A. *Control and Optimization of Multiscale Process Systems*; Birkhäuser: Boston, 2008.

(3) Varshney, A.; Armaou, A. Multiscale optimization using hybrid PDE/kMC process systems with application to thin film growth. *Chem. Eng. Sci.* **2005**, *60*, 6780–6794.

(4) Edwards, S. F.; Wilkinson, D. R. The surface statistics of a granular aggregate. *Proc. R. Soc. London, Ser. A* **1982**, *381*, 17–31.

(5) Villain, J. Continuum models of crystal growth from atomic beams with and without desorption. *J. Phys. I* **1991**, *1*, 19–42.

(6) Vvedensky, D. D.; Zangwill, A.; Luse, C. N.; Wilby, M. R. Stochastic equations of motion for epitaxial growth. *Phys. Rev. E* **1993**, *48*, 852–862.

(7) Cuerno, R.; Makse, H. A.; Tomassone, S.; Harrington, S. T.; Stanley, H. E. Stochastic Model for Surface Erosion via Ion Sputtering: Dynamical Evolution from Ripple Morphology to Rough Morphology. *Phys. Rev. Lett.* **1995**, *75*, 4464–4467.

(8) Lauritsen, K. B.; Cuerno, R.; Makse, H. A. Noisy Kuramoto-Sivashinsky equation for an erosion model. *Phys. Rev. E* **1996**, *54*, 3577–3580.

(9) Lou, Y.; Christofides, P. D. Feedback Control of Surface Roughness Using Stochastic PDEs. *AIChE J.* **2005**, *51*, 345–352.

(10) Ni, D.; Christofides, P. D. Multivariable Predictive Control of Thin Film Deposition Using a Stochastic PDE Model. *Ind. Eng. Chem. Res.* **2005**, *44*, 2416–2427.

(11) Hu, G.; Lou, Y.; Christofides, P. D. Dynamic Output Feedback Covariance Control of Stochastic Dissipative Partial Differential Equations. *Chem. Eng. Sci.* **2008**, *63*, 4531–4542.

(12) Lou, Y.; Christofides, P. D. Nonlinear Feedback Control of Surface Roughness Using a Stochastic PDE: Design and Application to a Sputtering Process. *Ind. Eng. Chem. Res.* **2006**, *45*, 7177–7189.

(13) Lou, Y.; Hu, G.; Christofides, P. D. Model Predictive Control of Nonlinear Stochastic Partial Differential Equations with Application to a Sputtering Process. *AIChE J.* **2008**, *54*, 2065–2081.

(14) Levine, S. W.; Engstrom, J. R.; Clancy, P. A kinetic Monte Carlo study of the growth of Si on Si(100) at varying angles of incident deposition. *Surf. Sci.* **1998**, *401*, 112–123.

(15) Zhang, P.; Zheng, X.; Wu, S.; Liu, J.; He, D. Kinetic Monte Carlo simulation of Cu thin film growth. *Vacuum* **2004**, *72*, 405–410.

(16) Levine, S. W.; Clancy, P. A simple model for the growth of polycrystalline Si using the kinetic Monte Carlo simulation. *Model. Simul. Mater. Sci. Eng.* **2000**, *8*, 751–762.

(17) Wang, L.; Clancy, P. Kinetic Monte Carlo simulation of the growth of polycrystalline Cu films. *Surf. Sci.* **2001**, *473*, 25–38.

(18) Hu, G.; Orkoulas, G.; Christofides, P. D. Modeling and Control of Film Porosity in Thin Film Deposition. *Chem. Eng. Sci.* **2009**, *64*, 3668–3682.

(19) Hu, G.; Orkoulas, G.; Christofides, P. D. Regulation of Film Thickness, Surface Roughness and Porosity in Thin Film Growth Using Deposition Rate. *Chem. Eng. Sci.* **2009**, *64*, 3903–3913.

(20) Kleijn, C. R.; van der Meer, T. H.; Hoogendoorn, C. J. A Mathematical Model for LPCVD in a Single Wafer Reactor. *J. Electrochem. Soc.* **1989**, *11*, 3423–3433.

(21) Hu, G.; Orkoulas, G.; Christofides, P. D. Stochastic Modeling and Simultaneous Regulation of Surface Roughness and Porosity in Thin Film Deposition. *Ind. Eng. Chem. Res.* **2009**, *48*, 6690–6700.

(22) Yang, Y. G.; Johnson, R. A.; Wadley, H. N. A Monte Carlo simulation of the physical vapor deposition of nickel. *Acta Mater.* **1997**, *45*, 1455–1468.

(23) Hu, G.; Huang, J.; Orkoulas, G.; Christofides, P. D. Investigation of Film Surface Roughness and Porosity Dependence on Lattice Size in a Porous Thin Film Deposition Process. *Phys. Rev. E* **2009**, *80*, 041122.

Received for review September 7, 2009
Revised manuscript received October 23, 2009
Accepted October 27, 2009

IE901396G